ACS APPLIED MATERIALS & INTERFACES

Research Article

www.acsami.org

In Situ Biosynthesis of Fluorescent Platinum Nanoclusters: Toward Self-Bioimaging-Guided Cancer Theranostics

Donghua Chen,[†,‡,⊥] Chunqiu Zhao,[†,⊥] Jing Ye,[†] Qiwei Li,[†] Xiaoli Liu,[†] Meina Su,[†] Hui Jiang,[†] Christian Amatore,[§] Matthias Selke,[∥] and Xuemei Wang*[,†]

[†]State Key Laboratory of Bioelectronics (Chien-Shiung Wu Lab), School of Biological Science and Medical Engineering, Southeast University, Nanjing 210096, China

[‡]School of Chemistry and Chemical Engineering, Southeast University, Nanjing 211189, China

[§]CNRS UMR 8640 PASTEUR and LIA NanoBioCatEchem, Ecole Normale Supérieure-PSL Research University, Département de Chimie, Sorbonne Universités—UPMC Paris 6, 24 rue Lhomond, 75005 Paris, France

[∥]Department of Chemistry and Biochemistry, California State University, Los Angeles, California 90032, United States

Supporting Information

ABSTRACT: Among the noble-metal clusters, very few reports about platinum clusters were used as bioimaging probes of tumors except as a reducing catalyst. It is first established herein that the biocompatible platinum nanoclusters are spontaneously biosynthesized by cancerous cells (i.e., HepG2 (human hepatocarcinoma), A549 (lung cancer), and others) rather than noncancerous cells (i.e., L02 (human embryo liver cells)) when incubated with micromolar chloroplatinic acid solutions. These in situ biosynthesized platinum nanoclusters could be readily realized in a biological environment and emit a bright fluorescence at 460 nm, which could be further utilized to facilitate an excellent cancer-cell-killing efficiency when combined with porphyrin derivatives for photothermal treatment. This raises the possibility of providing a promising and precise bioimaging strategy for specific fluorescent self-biomarking of tumor locations and realizing fluorescence imaging-guided photothermal therapy of tumors.

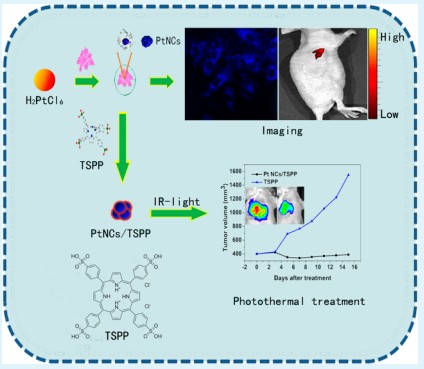

KEYWORDS: *platinum nanoclusters, cancer, theranostics, bioimaging, photothermal treatment*

INTRODUCTION

Despite improvement of the survival rates of cancer patients over the past few decades, cancer still remains one of the major causes of mortality, and the incidence of cancer continues to increase.[1] Effective diagnostic strategies in the early stages of cancer are critical and result in a high chance of an efficient cure. Medical imaging has become an indispensable tool in the field of early tumor diagnosis, and in vivo fluorescence imaging of tumor locations may accurately localize the diseased sites for direct bioimaging of tumors and for precise monitoring of specific treatment processes.[2−4] Our recent studies demonstrate that biosynthesized fluorescent gold or silver nanoclusters (NCs) can be readily utilized as a potential probe for highly sensitive optical imaging of cancer on both the cellular and the animal levels.[5,6]

It is well-known that tumors have relatively low oxygen concentration levels, and therefore a more reducing environment compared to normal tissue. The reductive microenvironment of hypoxic tumors is also related to insufficient formation of new blood vessels during growth.[7,8] Furthermore, compared to normal cells, cancerous cells exhibit a relatively high amount of GSH−GSSG, NAD(P)H, and cysteine-containing proteins to cope with the high productions of reactive oxygen (ROS) or nitrogen (RNS) species by cancer cells and tumors to maintain the cellular redox homeostasis. As a result of these properties, an oxidizing species such as Pt(IV) actually shows the highest activity in vivo.[9]

In addition to being a main antitumor agent for many years, platinum has recently drawn interest as a specific biomarker in its insoluble forms. In particular, nonclassical platinum(IV) antitumor complexes with octahedral structures have been found to exhibit low side effects in the gastrointestinal tract and blood when administered orally.[9,10] However, conventional platinum fluorophores for bioimaging applications often suffer from poor photostability, rapid photobleaching, and especially aggregation and high plasma protein binding rates, and thus cannot be used for long-term bioimaging. Furthermore, sensitivity may be limited during bioimaging processes owing to the limited number of fluorophores conjugated per ligand.[11] In situ self-bioimaging of cancer cells and tumor tissues through their spontaneous ability to biosynthesize specific fluorescent NCs may overcome this significant difficulty. Recent reports have shown platinum nanoparticles can be generated in plants, bacteria, fungi, and yeasts following absorption of platinum

Received: June 29, 2015
Accepted: July 31, 2015
Published: July 31, 2015

DOI: 10.1021/acsami.5b05805
ACS Appl. Mater. Interfaces 2015, 7, 18163−18169

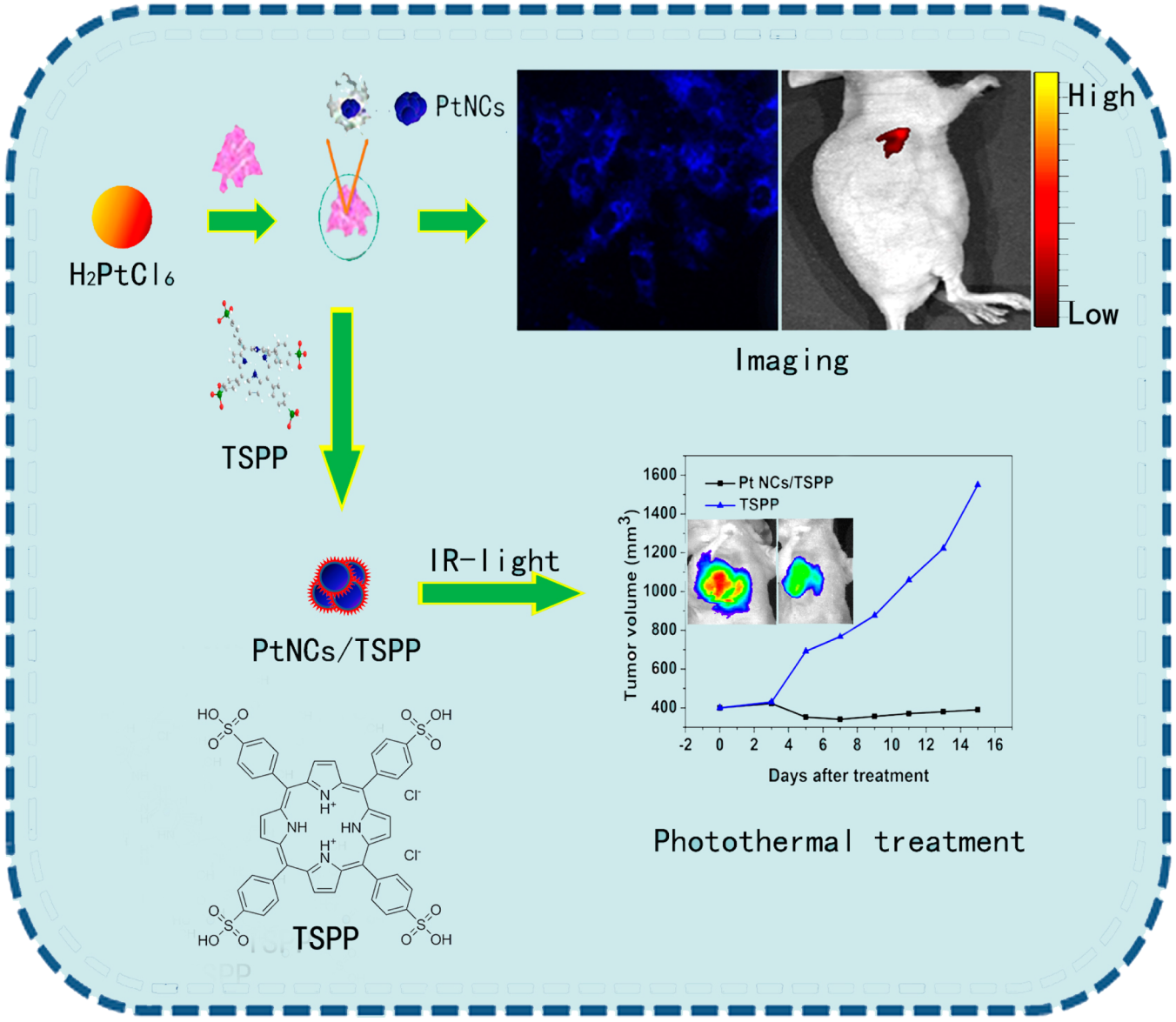

Figure 1. Schematic illustration of the study rationale and design.

ions.[12−15] This bioreduction of metal salts into metallic nanoparticles acts as an organism's survival mechanism against toxic metal ions and occurs via an active or passive process or a combination of the two.[16,17] Indeed, we have recently reported in situ synthesis of fluorescent gold/silver nanoclusters in tumor cells for target tumor imaging.[5,6] In this study, we explore the possibility of in situ biosynthesis of fluorescent platinum nanoclusters in cancer cells or tumor tissues for precise in vivo self-bioimaging of tumor locations and thereby developing a fluorescence-guided treatment of target tumors. This study demonstrates that when cancerous cells biosynthesized in situ are cultured with micromolar chloroplatinic acid solutions, the resulting biocompatible platinum nanoclusters exhibit fluorescence which is suitable for bioimaging. Furthermore, in vivo imaging of a xenografted tumor in nude mice also established the validity of this strategy for rapid and precise targeting as well as bioimaging of tumors by subcutaneous injections or via intravenous injection of chloroplatinic acid solutions, without significant dissemination to the surrounding normal tissues. The mechanism by which cancerous cells (in cultures or in tumors) reduce the Pt(IV) moieties into metallic nanoclusters still remains unknown. However, since the same does not occur in normal cells or tissues,[5,6] the biosynthetic process appears to correlate with the high inflammatory status of cancer cells, viz., with the fact that their high metabolisms involve a much larger production of chemical reductants.[8,16] In the absence of easily reducible metal ions such as Pt(IV), this excess of reductants is removed via reduction of dioxygen, leading to the formation of reactive oxygen and nitrogen species. In our view, the in situ biosynthesis from chloroplatinic acid into platinum nanoclusters thus short-circuits the natural mechanisms operating in cancer cells to eliminate the oxidative stress incurred by their high metabolic activity.

Photothermal therapy (PTT), as a potential therapeutic strategy in tumor treatments, has been well-known for the past few decades.[18,19] Porphyrins and derivatives are good candidates as photosensitizers (PSs) for use in photodynamic therapy (PDT) or PTT treatment.[20−22] Metal nanoparticles such as gold nanoparticles[23−25] and platinum nanoparticles[26,27]

DOI: 10.1021/acsami.5b05805
ACS Appl. Mater. Interfaces 2015, 7, 18163−18169

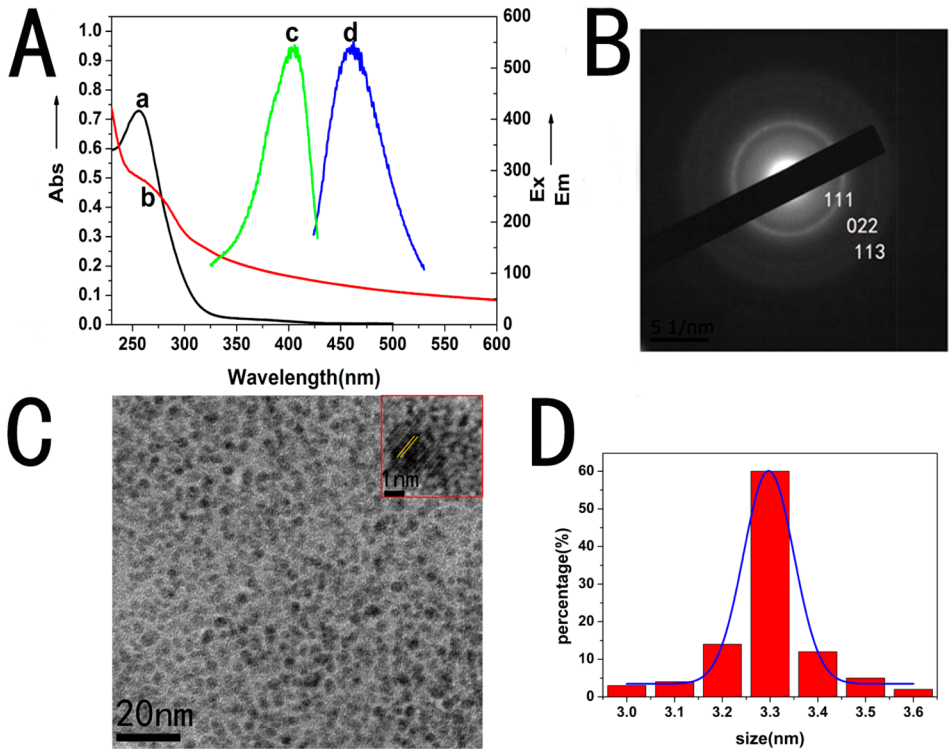

Figure 2. (A) Optical microscopy characterization of platinum nanoclusters biosynthesized in situ by HepG2 cancer cells after their incubation with H_2PtCl_6 (0.25 mmol/L) for 24 h: (a, b) UV−vis absorption spectra of H_2PtCl_6 and the relevant platinum nanoclusters, (c) excitation spectrum, (d) fluorescence emission spectrum (Em) with excitation at 405 nm. (B) Selected area electron diffraction of platinum nanoclusters. (C) TEM image of biosynthesized Pt nanoclusters, showing the 0.21 nm interplanar spacing of the platinum nanoclusters (inset). (D) Hydrodynamic diameter measured using DLS (mean value ca. 3.3 nm).

have recently been reported as potential PSs for PTT, but these conventional metal nanoparticles prepared with chemical modifications may exhibit inherent problems such as toxicity, low accumulation in cancer cells, fast elimination and accumulation in the liver and kidneys, etc., and thus may not be useful for efficient PSs in PTT. We have therefore explored the possible use of the in situ biosynthesis of fluorescent platinum nanoclusters (Pt NCs) in cancer cells (i.e., HepG2 (human hepatocarcinoma), A549 (lung cancer), HeLa (cervical cancer), HCT-116 (colon cancer), etc.) and tumor tissues via their spontaneous self-building through metallic salt reduction that certainly results from the fact that cancer cells have a different redox homeostasis than normal cells. Moreover, we have combined the spontaneous intracellular formation of fluorescent platinum nanoclusters with a photothermal treatment of tumors by using the water-soluble porphyrin tetrakis(sulfonatophenyl)porphyrin (TSPP), leading to synergistic effects and enhancement of the therapeutic efficacy of IR irradiation, and thus providing a new strategy for effective fluorescence imaging and guided photothermal therapy of tumors. See Figure 1 for an illustration of the study design.

EXPERIMENTAL SECTION

Characterization of in Situ Biosynthesized Pt NCs in Cells. Pt NCs were biosynthesized in situ through incubation of different cell lines, including cancer cells such as HepG2, HeLa, or A549 cells, with various concentrations of H_2PtCl_6 added to the usual cells under culturing conditions. After 24 or 48 h of incubation, the biosynthesized Pt NCs extracted from incubated cancer cells by a repetitive freeze−thaw method were characterized by a UV−vis−NIR spectrophotometer (Shimadzu, UV3600) and a fluorescence spectrometer (PerkinElmer, LS-55).

The cells interspersed with Pt NCs which were immobilized on an indium−tin oxide (ITO) glass substrate were measured by a field-emission scanning electron microscope (Zeiss, Ultra Plus). A transmission electron microscope (JEM-2100) was used to characterize the size as well as the size distribution of Pt NCs. An X-ray photoelectron spectrometer (PHI 5000, VersaProbe) was used to investigate the valence state of platinum atoms in the in situ biosynthesis of Pt NCs.

In Situ and in Vivo Bioimaging Study. HepG2, HeLa, HCT-116, A549, or L02 cells were treated with different concentrations of H_2PtCl_6 solutions for cellular imaging and incubated at 37 °C for 24 or 48 h. Before fluorescence imaging, the cells were washed three times with PBS. A 405 nm excitation laser (Andor Revolution XD) was focused using a 20× IR coated objective (Nikon).

For in vivo bioimaging of Pt NCs in the tumor, the xenograft tumor mice were injected near the tumor location or through the mouse tails with a 5 mmol/L H_2PtCl_6 solution (100 μL). By inhalation of a mixture of oxygen with isoflurane (5%), the mice were fully anesthetized at different times postinjection. The in vivo bioimages were acquired on a Cri Maestroin and PerkinElmer in vivo imaging system (excitation, 420−440 nm; emission, 570−620 nm). The ROI (regions of interest) analysis was measured by using the CRi Maestro Image software. The studies were approved by the National Institute of Biological Science and Animal Care Research Advisory Committee of Southeast University, and experiments were conducted following the guidelines of the Animal Research Ethics Board of Southeast University.

RESULTS AND DISCUSSION

Different kinds of cancer cell lines (i.e., HepG2 (human hepatocarcinoma), A549 (lung cancer), HeLa (cervical cancer), HCT-116 (colon cancer), etc.) were selected as models to evaluate the pertinence of platinum NCs spontaneously biosynthesized in situ by cancer cells. For comparison, normal

DOI: 10.1021/acsami.5b05805
ACS Appl. Mater. Interfaces 2015, 7, 18163−18169

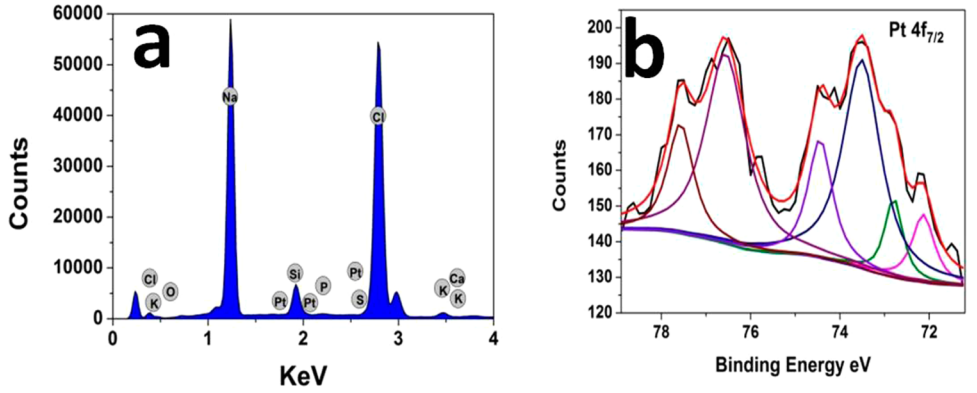

Figure 3. (a) EDS spectrum of the platinum nanoclusters biosynthesized in situ by HepG2 cancer cells after 24 h of incubation with H_2PtCl_6. (b) X-ray photoelectron spectra evidencing the Pt 4f photoelectron emission from platinum nanoclusters biosynthesized in situ by HepG2 cells after 24 h of incubation with H_2PtCl_6.

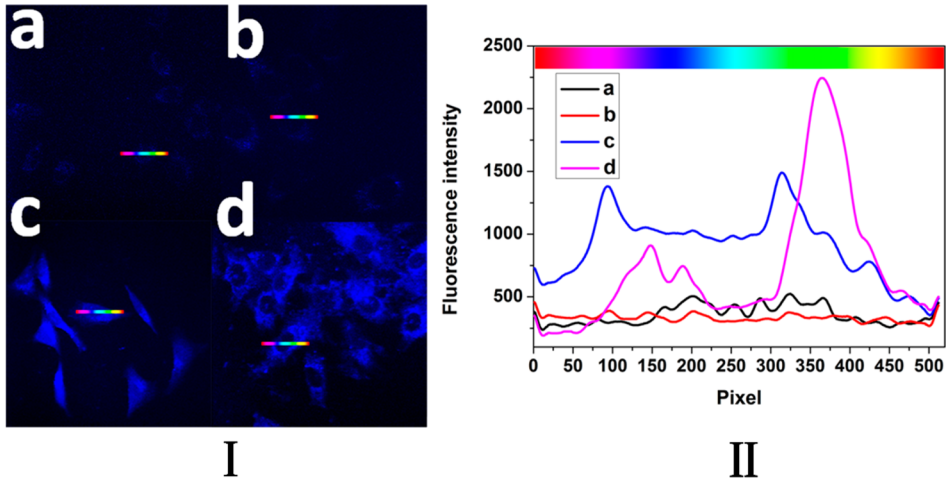

Figure 4. (I) Laser confocal fluorescence micrographs of L02 control cells (a) and HepG2 cells (b) incubated with DMEM in the absence of 0.25 mmol/L H_2PtCl_6 solutions for 24 h. Laser confocal fluorescence micrographs of HepG2 (c) cells and A549 cells (d) incubated with DMEM in the presence of 0.25 mmol/L H_2PtCl_6 solutions for 24 h. (II) Relative fluorescence intensity variations along cross-sections of relevant cells in (I): (a) in panel I, part a, (b) in panel I, part b, (c) in panel I, part c, (d) in panel I, part d (the color gradient coding illustrates the direction of the sampling in (I)).

cell lines (i.e., L02 liver cells) were used as controls. The cancer cells were incubated for 24 or 48 h with chloroplatinic acid biocompatible salts. Note that the absence of cytotoxicity of chloroplatinic acid in cells was confirmed and measured by MTT assay (Figure S1). The intracellular presence of biosynthesized platinum NCs formed inside the cells was observed by UV−vis absorption spectroscopy, fluorescence spectroscopy, transmission electron microscopy (TEM) together with selected area electron diffraction (SAED) for transmission electron microscopes and energy-dispersive spectroscopy (EDS), and X-ray photoelectron spectroscopy (XPS). In the case of cancer cells, including HepG2 cells and others, when incubated with chloroplatinic acid solutions, the biosynthesized Pt NCs displayed excitation and emission wavelengths of 404 and 460 nm, respectively, in agreement with the fluorescence at 420 and 470 nm previously reported by Tanaka[28] and Kawasaki.[29] The emission wavelength is also very close to the emission wavelength of 456 nm for platinum nanoparticle sols synthesized by chemical etching by GSH,[30] suggesting that the final NCs may be capped with sulfydryl groups. Compared with chloroplatinic acid, UV−vis absorption spectra displayed a weak peak at 260 nm, indicating that a few Pt(IV) metal centers were still present, though most of them had been reduced to lower valence states (Figure 2A). Our observations of selected areas of the platinum nanoclusters by electron diffraction established that multiple platinum nanocrystals were biosynthesized in situ by the cancer cells. Some very weak diffraction peaks corresponding to some crystal faces indicated *d*-spacing values of 0.212, 0.133, and 0.112 nm that match reflection from Pt(111), Pt(022), and Pt(113) planes, and HR-TEM established that the biosynthesized Pt NCs involved platinum atom planes with an interplane distance of ca. 0.21 nm, corresponding to Pt(111), yet the spherical platinum nanoparticles were amorphous to electron diffraction[14] (Figure 2B). TEM analysis indicated that 98% of the Pt NCs ranged between 3.0 to 3.6 nm in diameter with a distribution peak at 3.3 nm (Figure 2C), which were almost spherical and had no noticeable trend to agglomerate (Figure 2C, inset). As shown in Figure 3, the EDS results indicate that there are no other elemental impurities present in the biosynthesized nanoparticles. To further confirm the formation and valence state of the Pt NCs inside the cancer cells, we recorded high-resolution XPS spectra of Pt 4f. The deconvoluted Pt 4f spectrum was composed of three spin−

DOI: 10.1021/acsami.5b05805
ACS Appl. Mater. Interfaces 2015, 7, 18163−18169

orbit doublets with the Pt $4f_{7/2}$ components at 72.1, 72.8, and 73.5 eV, attributed to Pt(0), Pt(II), and Pt(IV) phases, respectively,[30,31] thus suggesting successful formation of platinum nanoclusters composed of Pt domains with different oxidation states. In agreement with this result, quantitative analysis indicated Pt(0):Pt(II):Pt(IV) atomic concentration ratios of 1.1:1.0:5.4, consistent with nanocluster structures involving a metallic Pt(0) core decorated by Pt(II)- and Pt(IV)-containing phases.

The bright blue fluorescence of platinum nanoclusters biosynthesized in situ inside different cancer cells appears to be adequate for their use for in vivo bioimaging of live tumor cells. In this study, confocal fluorescence microscopy (Leica TCS SP2) measurements at an excitation wavelength of 405 nm were used to assess the potential for bioimaging of cancer cells treated with aqueous H_2PtCl_6. As expected, intracellular fluorescence was clearly observable after the HeLa, HepG2, A549, and HCT-116 cancer cells were incubated for 24 h with 0.25 mmol/L H_2PtCl_6 (Figure 4, Figure S2). This was further confirmed by comparison of the quantitative spatial variations in the fluorescence intensities across the cells for the test groups and control groups, as shown in Figure 4, panel II. No detectable fluorescence signal was observed when the same cells were treated with DMEM/high-glucose medium. More importantly, comparatively very weak fluorescence signals could be observed when various concentrations of H_2PtCl_6 were added to noncancerous cells cultures (i.e., L02 cells), indicating that biosynthesis of Pt nanoclusters from chloroplatinic acid solutions could not occur as efficiently in noncancerous cells, thus allowing kinetically controlled selective imaging by fluorescence microscopy.

The above results established the in situ validity of the present approach, forcing cancer cells to spontaneously produce and confine self-imaging fluorescent markers when incubated with chloroplatinic acid solutions. We then explored the possible use of in vivo fluorescence imaging of tumors based on in situ biosynthesized fluorescent Pt NCs. For this purpose, we relied on a xenograft tumor model of cervical carcinoma or colorectal carcinoma in nude mice. As shown in Figure 5, Figure 6, and Figure S3, intravenous injection through the mouse tails or subcutaneous injection of chloroplatinic acid solution (0.1 mL, 5 mmol/L H_2PtCl_6) around xenograft tumors allowed the clear observation of bright fluorescence around the tumor after 24 h. Conversely, control mice did not exhibit any

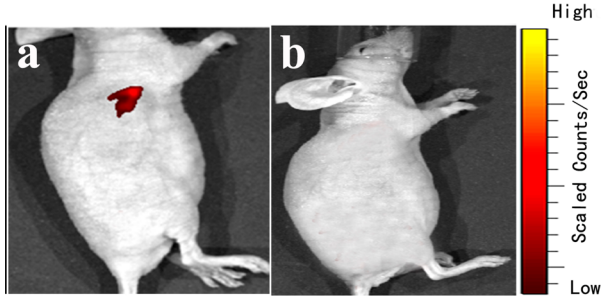

Figure 5. Representative xenograft tumor mouse models of HeLa cells observed by in vivo fluorescence imaging. (a) Xenograft tumor mouse model of HeLa cells by in vivo fluorescence imaging 24 h after a subcutaneous injection of 0.1 mL of a 5 mmol/L H_2PtCl_6 solution near the tumor. (b) Control mouse observed by in vivo fluorescence imaging 24 h after a subcutaneous injection of 0.1 mL of a 5 mmol/L H_2PtCl_6 solution in the right side of its abdomen.

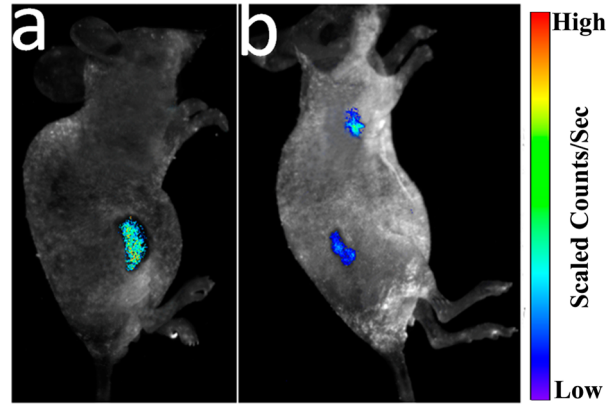

Figure 6. Fluorescence detection of (a) a xenograft tumor mouse model of HCT-116 cells where the mouse lies on its left side or (b) a xenograft tumor mouse model of HeLa cells (axillary subcutaneous) and HCT-116 cells (the lateral thigh) where the mouse lies with the back below for its top part and on the left side for its bottom section by tilting of its spine around the waist, observed by in vivo fluorescence imaging 24 h after an intravenous injection of 0.1 mL of a 5 mmol/L H_2PtCl_6 solution through the mouse tails.

fluorescent areas 24 h after subcutaneous or intravenous injection of chloroplatinic acid solution (0.1 mL, 5 mmol/L H_2PtCl_6) in the right side of their abdomen. This indicated that cancer cells present in tumors could readily absorb and reduce Pt(IV) ions into Pt NCs as in in situ experiments, while this could not occur inside noncancerous tissues. The ex vivo observation of the excised tumors closely correlated with the in vivo imaging, confirming that most of the fluorescence originated from the tumor tissues, while little or low fluorescence arose from surrounding tissues or from visceral organs such as the liver, kidney, and others (Figure S4). In addition, in each category (i.e., with or without xenografted tumors) the mice submitted to the chloroplatinic treatments did not evidence any changes in eating, drinking, exploratory behavior, activity, physical features, and neurological status compared to control mice, confirming the good biocompatibility of chloroplatinic acid solutions and the absence of obvious toxic effects.

On the basis of the above study, we further explored the possibility of the synergistic effect on photothermal therapy of tumors by using biosynthesized platinum nanoclusters through combination with TSPP, a potential PTT agent. As shown in Figure S4, 24 h after subcutaneous injection of a H_2PtCl_6 solution (0.1 mL, 2.5 mmol/L) of TSPP (0.1 mL, 0.1 μg/mL) near the tumor, fluorescence could be readily detected by using the Cri Maestro in vivo imaging system. Compared with the control group (i.e., injection of H_2PtCl_6 alone or TSPP alone), the fluorescence intensity in the biosynthesized platinum nanoclusters combined with TSPP significantly changed (Figure S5), suggesting that TSPP may readily interact with the biosynthesized platinum nanoclusters in tumors and further enhance the relevant treatment efficacy. As shown in Figure 7, the synergistic effect on photothermal therapy of tumors by using biosynthesized platinum nanoclusters in combination with TSPP could readily be assessed by comparison of the tumor growth and the survival period between the relevant experimental mice exposed to infrared (IR) irradiation by using biosynthesized platinum nanoclusters and TSPP as well as other control mice. This provides evidence that the tumors xenografted in mice treated by the combination of biosynthe-

DOI: 10.1021/acsami.5b05805
ACS Appl. Mater. Interfaces 2015, 7, 18163−18169

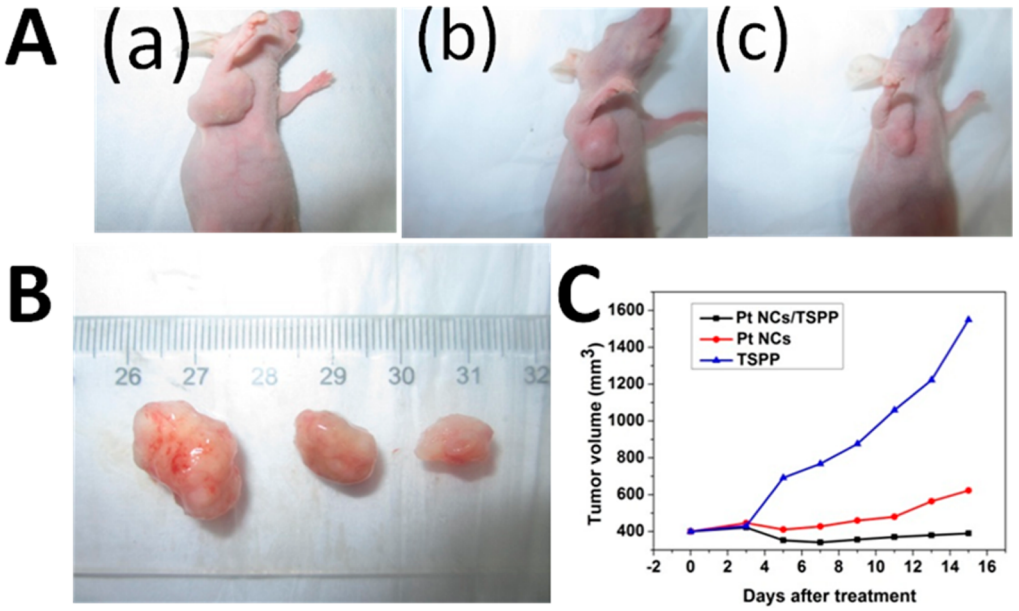

Figure 7. (A) Photographs of mice 15 days after treatment. The mice were exposed to 635 nm LED light 24 h after injection of (a) TSPP alone, (b) H_2PtCl_6 alone (viz., with tumors exposed to biosynthesized platinum nanoclusters alone), and (c) TSPP and H_2PtCl_6. (B) Excised tumors from mice shown as (a), (b), and (c) in (A) from left to right. (C) Mean tumor growth kinetics as a function of treatment.

sized platinum nanoclusters and TSPP had been reduced to a much smaller size than those of control mice and that tumor growth was significantly inhibited after 15 days. Furthermore, all treated mice were in good health condition, while those from the control groups were very emaciated or had passed away during this period. These results demonstrated that the combination of precise biomarking by the platinum nanocluster for in vivo fluorescent self-biomarking of tumor locations with photothermal treatment of tumors can readily provide a synergistic effect and thus lead to a fluorescence-imaging-guided photothermal therapy of tumors.

CONCLUSIONS

In summary, our observations demonstrate the ability of tumor cells under both in situ (cell cultures) and in vivo (xenografted tumors in nude mice) conditions to rapidly biosynthesize Pt NCs upon exposure to aqueous chloroplatinic solutions, while this did not occur as fast in normal cells and tissues (controls). The reduction of Pt(IV) appears to stem from the increased reducing capacity of cancer cells via their propensity to generate H_2O_2 and ROS through dioxygen reductions. This leads to an easy and inoffensive procedure for self-marking of cancer cells and tumors by spontaneous fluorescence bioimaging. On the other hand, combining such treatment with injection of photosensitizers such as TSPP provides an efficient method for fluorescence-imaging-guided photothermal therapy of cancers.

ASSOCIATED CONTENT

Supporting Information

The Supporting Information is available free of charge on the ACS Publications website at DOI: 10.1021/acsami.5b05805.

Experimental details and results of MTT assay assessment, laser confocal fluorescence micrographs of L02 control cells, A549 cells, and HCT-116 cells incubated with or without H_2PtCl_6 solutions, representative xenograft tumor mouse models of HeLa cells and relevant mean fluorescence intensity observed by in vivo fluorescence imaging, and representative ex vivo fluorescence images of excised HeLa tumors and other visceral organs from H_2PtCl_6-injected xenograft tumor mouse (PDF)

AUTHOR INFORMATION

Corresponding Author

* E-mail: xuewang@seu.edu.cn. Phone: +86-25-83792177.

Author Contributions

⊥D.C. and C.Z. contributed equally to this work.

Notes

The authors declare no competing financial interest.

ACKNOWLEDGMENTS

This work is supported by the National Natural Science Foundation of China (Grant 81325011), National High Technology Research & Development Program of China (Grants 2015AA020502 and 2012AA022703), and Major Science & Technology Project of Suzhou (Grant ZXY2012028). C.A. acknowledges support from UMR 8640 (Grant ENS-CNRS-UPMC) and LIA NanoBioCatEchem. M.Se. acknowledges support from the NSF-CREST program (NSF Grant HRD-0932421).

REFERENCES

(1) Siegel, R.; Naishadham, D.; Jemal, A. Cancer Statistics, 2013. *Ca-Cancer J. Clin.* **2013**, *63*, 11−30.

(2) Wu, X.; Sun, X.; Guo, Z.; Tang, J.; Shen, Y.; James, T. D.; Tian, H.; Zhu, W. *In Vivo* and *In Situ* Tracking Cancer Chemotherapy by Highly Photostable NIR Fluorescent Theranostic Prodrug. *J. Am. Chem. Soc.* **2014**, *136*, 3579−88.

(3) Sun, X.; Huang, X.; Guo, J.; Zhu, W.; Ding, Y.; Niu, G.; Wang, A.; Kiesewetter, D. O.; Wang, Z. L.; Sun, S.; Chen, X. Self-Illuminating 64Cu-Doped Cdse/Zns Nanocrystals for *In Vivo* Tumor Imaging. *J. Am. Chem. Soc.* **2014**, *136*, 1706−9.

(4) Robinson, J. T.; Hong, G.; Liang, Y.; Zhang, B.; Yaghi, O. K.; Dai, H. *In Vivo* Fluorescence Imaging in the Second Near-Infrared Window

DOI: 10.1021/acsami.5b05805
ACS Appl. Mater. Interfaces 2015, 7, 18163−18169

with Long Circulating Carbon Nanotubes Capable of Ultrahigh Tumor Uptake. *J. Am. Chem. Soc.* **2012**, *134*, 10664−9.
(5) Wang, J.; Zhang, G.; Li, Q.; Jiang, H.; Liu, C.; Amatore, C.; Wang, X. *In Vivo* Self-Bio-Imaging of Tumors Through in Situ Biosynthesized Fluorescent Gold Nanoclusters. *Sci. Rep.* **2013**, *3*, 1157.
(6) Gao, S.; Chen, D.; Li, Q.; Ye, J.; Jiang, H.; Amatore, C.; Wang, X. Near-Infrared Fluorescence Imaging of Cancer Cells and Tumors Through Specific Biosynthesis of Silver Nanoclusters. *Sci. Rep.* **2014**, *4*, 4384.
(7) Reisner, E.; Arion, V. B.; Keppler, B. K.; Pombeiro, A. J. L. Electron-Transfer Activated Metal-Based Anticancer Drugs. *Inorg. Chim. Acta* **2008**, *361*, 1569−1583.
(8) Ben-Baruch, A. The Tumor-Promoting Flow of Cells Into, Within and Out of the Tumor Site: Regulation by the Inflammatory Axis of TNFa and Chemokines. *Cancer Microenviron.* **2012**, *5*, 151−164.
(9) Graf, N.; Lippard, S. J. Redox Activation of Metal-Based Prodrugs as A Strategy for Drug Delivery. *Adv. Drug Delivery Rev.* **2012**, *64*, 993−1004.
(10) Min, Y.; Li, J.; Liu, F.; Yeow, E. K.; Xing, B. Near-Infrared Light-Mediated Photoactivation of A Platinum Antitumor Prodrug and Simultaneous Cellular Apoptosis Imaging by Upconversion-Luminescent Nanoparticles. *Angew. Chem., Int. Ed.* **2014**, *53*, 1012−1016.
(11) Mazumder, S.; Dey, R.; Mitra, M. K.; Mukherjee, S.; Das, G. C. Review: Biofunctionalized Quantum Dots in Biology and Medicine. *J. Nanomater.* **2009**, *2009*, 1−17.
(12) Bali, R.; Siegele, R.; Harris, A. T. Biogenic Pt Uptake and Nanoparticle Formation in Medicago Sativa and Brassica Juncea. *J. Nanopart. Res.* **2010**, *12*, 3087−3095.
(13) Riddin, T. L.; Gericke, M.; Whiteley, C. G. Analysis of the Inter- And Extracellular Formation of Platinum Nanoparticles by Fusarium Oxysporum F. Sp. Lycopersici Using Response Surface Methodology. *Nanotechnology* **2006**, *17*, 3482−9.
(14) Lengke, M. F.; Fleet, M. E.; Southam, G. Synthesis of Platinum Nanoparticles by Reaction of Filamentous Cyanobacteria with Platinum(IV)-Chloride Complex. *Langmuir* **2006**, *22*, 7318−23.
(15) Konishi, Y.; Ohno, K.; Saitoh, N.; Nomura, T.; Nagamine, S.; Hishida, H.; Takahashi, Y.; Uruga, T. Bioreductive Deposition of Platinum Nanoparticles on the Bacterium Shewanella Algae. *J. Biotechnol.* **2007**, *128*, 648−53.
(16) Amatore, C.; Arbault, S.; Guille, M.; Lemaître, F. Electrochemical Monitoring of Single Cell Secretion: Vesicular Exocytosis and Oxidative Stress. *Chem. Rev.* **2008**, *108*, 2585−2621.
(17) Jung, H. S.; Han, J.; Lee, J. H.; Lee, J. H.; Choi, J. M.; Kweon, H. S.; Han, J. H.; Kim, J. H.; Byun, K. M.; Jung, J. H.; Kang, C.; Kim, J. S. Enhanced NIR Radiation-Triggered Hyperthermia by Mitochondrial Targeting. *J. Am. Chem. Soc.* **2015**, *137*, 3017−23.
(18) Jiang, B. P.; Hu, L. F.; Shen, X. C.; Ji, S. C.; Shi, Z.; Liu, C. J.; Zhang, L.; Liang, H. One-Step Preparation of A Water-Soluble Carbon Nanohorn/Phthalocyanine Hybrid for Dual-Modality Photothermal and Photodynamic Therapy. *ACS Appl. Mater. Interfaces* **2014**, *6*, 18008−17.
(19) Chen, Q.; Wang, C.; Zhan, Z.; He, W.; Cheng, Z.; Li, Y.; Liu, Z. Near-Infrared Dye Bound Albumin with Separated Imaging and Therapy Wavelength Channels for Imaging-Guided Photothermal Therapy. *Biomaterials* **2014**, *35*, 8206−14.
(20) Jin, C. S.; Lovell, J. F.; Chen, J.; Zheng, G. Ablation of Hypoxic Tumors with Dose-Equivalent Photothermal, but not Photodynamic, Therapy using A Nanostructured Porphyrin Assembly. *ACS Nano* **2013**, *7*, 2541−50.
(21) Hayashi, K.; Nakamura, M.; Miki, H.; Ozaki, S.; Abe, M.; Matsumoto, T.; Kori, T.; Ishimura, K. Photostable Iodinated Silica/Porphyrin Hybrid Nanoparticles with Heavy-Atom Effect for Wide-Field Photodynamic/Photothermal Therapy using Single Light Source. *Adv. Funct. Mater.* **2014**, *24*, 503−513.
(22) Xu, J.; Zeng, F.; Wu, H.; Yu, C.; Wu, S. Dual-Targeting Nanosystem for Enhancing Photodynamic Therapy Efficiency. *ACS Appl. Mater. Interfaces* **2015**, *7*, 9287−96.
(23) Melancon, M. P.; Lu, W.; Yang, Z.; Zhang, R.; Cheng, Z.; Elliot, A. M.; Stafford, J.; Olson, T.; Zhang, J. Z.; Li, C. *In Vitro* and *In Vivo* Targeting of Hollow Gold Nanoshells Directed at Epidermal Growth Factor Receptor for Photothermal Ablation Therapy. *Mol. Cancer Ther.* **2008**, *7*, 1730−9.
(24) Carpin, L. B.; Bickford, L. R.; Agollah, G.; Yu, T. K.; Schiff, R.; Li, Y.; Drezek, R. A. Immunoconjugated Gold Nanoshell-Mediated Photothermal Ablation of Trastuzumab-Resistant Breast Cancer Cells. *Breast Cancer Res. Treat.* **2011**, *125*, 27−34.
(25) Lu, W.; Melancon, M. P.; Xiong, C.; Huang, Q.; Elliott, A.; Song, S.; Zhang, R.; Flores, L. G., 2nd; Gelovani, J. G.; Wang, L. V.; Ku, G.; Stafford, R. J.; Li, C. Effects of Photoacoustic Imaging and Photothermal Ablation Therapy Mediated by Targeted Hollow Gold Nanospheres in An Orthotopic Mouse Xenograft Model of Glioma. *Cancer Res.* **2011**, *71*, 6116−21.
(26) Chen, D.; Gao, S.; Ge, W.; Li, Q.; Jiang, H.; Wang, X. One-Step Rapid Synthesis of Fluorescent Platinum Nanoclusters for Cellular Imaging and Photothermal Treatment. *RSC Adv.* **2014**, *4*, 40141.
(27) Manikandan, M.; Hasan, N.; Wu, H. F. Platinum Nanoparticles for The Photothermal Treatment of Neuro 2A Cancer Cells. *Biomaterials* **2013**, *34*, 5833−42.
(28) Tanaka, S.; Miyazaki, J.; Tiwari, D. K.; Jin, T.; Inouye, Y. Fluorescent Platinum Nanoclusters: Synthesis, Purification, Characterization, and Application to Bioimaging. *Angew. Chem., Int. Ed.* **2011**, *50*, 431−5.
(29) Kawasaki, H.; Yamamoto, H.; Fujimori, H.; Arakawa, R.; Inada, M.; Iwasaki, Y. Surfactant-Free Solution Synthesis of Fluorescent Platinum Subnanoclusters. *Chem. Commun. (Cambridge, U. K.)* **2010**, *46*, 3759−61.
(30) Le Guével, X.; Trouillet, V.; Spies, C.; Jung, G.; Schneider, M. Synthesis of Yellow-Emitting Platinum Nanoclusters by Ligand Etching. *J. Phys. Chem. C* **2012**, *116*, 6047−6051.
(31) Silva, J. C. M.; Souza, R. F. B. D.; Romano, M. A.; D'Villa-Silva, M.; Calegaro, M. L.; Hammer, P.; Neto, A. O.; Santos, M. C. Ptsnir/C Anode Electrocatalysts: Promoting Effect in Direct Ethanol Fuel Cells. *J. Braz. Chem. Soc.* **2012**, *23*, 1146−1153.

DOI: 10.1021/acsami.5b05805
ACS Appl. Mater. Interfaces 2015, 7, 18163−18169